(32)

Modeling the Effect of Boron on Microdefect Formation

by

Hendi Susanto

Submitted to the Department of Chemical Engineering
in partial fulfillment of the requirements for the degree of

Engineer in Chemical Engineering
at the

MASSACHUSETTS INSTITUTE OF TECHNOLOGY

September 1998

Author .....

Department of Chemical Engineering
September 11, 1998

Certified by .....

Robert A. Brown
Provost of MIT and
Warren K. Lewis Professor of Chemical Engineering

Accepted by .....

Robert E. Cohen
Chairman, Committee for Graduate Students

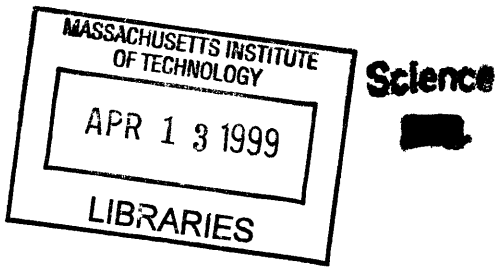

Modeling the Effect of Boron on Microdefect Formation

by

Hendi Susanto

Submitted to the Department of Chemical Engineering
on September 11, 1998, in partial fulfillment of the requirements for the degree of
Engineer in Chemical Engineering

Abstract

As microelectronic devices demand larger diameter wafers and reduced microdefect concentration and size, one of the most crucial issues in the semiconductor industry becomes the understanding of defect formation in silicon crystal growth by the Czochralski crystal growth method. Microdefect patterns in the crystal are known to be associated with the native point defects, namely self-interstitials and vacancies. The focus of this thesis is the analysis of the Oxidation Induced Stacking Fault Ring (OSF-Ring) which is known to correspond to a neutral region where the concentrations of the self-interstitials and vacancies are essentially in balance. The dynamics of the OSF-Ring with changes in crystal growth operating conditions, crystal growth rate and temperature field, has been explained quantitatively for crystals containing only self-interstitials and vacancies (Sinno, 1998). The neutral ring separates a core of vacancy rich crystal from a self-interstitial rich external ring. Microvoids form in the core by vacancy aggregation. Dislocation loops form in the self-interstitial rich region.

The presence of dopants in the crystal also affects microdefect distributions by interacting directly with self-interstitials and vacancies. At low dopant concentrations, the OSF-Ring position depends exclusively on the operating conditions. Crystal growth experiments by Dornberger et al. (1997) have shown the influence of high boron doping levels ($1x10^{15}$ - $2x10^{19}$ cm^{-3}) on the OSF-Ring position; high boron concentrations shift the OSF-Ring toward the center of the crystal without changes in growth conditions. The OSF-Ring diameter shrinks as a result of a shift of the point defect balance in favor of self-interstitials because of either vacancy depletion or self-interstitial addition.

The point defect dynamics model described by Sinno (1998) for silicon consists of point defect transport by Fickian diffusion and bulk crystal motion, and the consumption or generation of point defects by recombination. The crystal temperature field and crystal shape data was obtained from the heat transfer simulations of Dornberger et al. (1997b) for Czochralski crystal growth

systems. The intrinsic point defect model of Sinno (1998) was extended in this thesis to include boron-point defect interactions in the crystal. The following reactions are considered:

$$I + V \leftrightarrow 0, \quad (1)$$

$$B + B \leftrightarrow B_2, \quad (2)$$

$$B + I \leftrightarrow BI, \quad (3)$$

$$B_2 + I \leftrightarrow B_2I, \quad (4)$$

$$B + V \leftrightarrow BV, \quad (5)$$

$$BI + V \leftrightarrow B, \quad (6)$$

where I, V, 0, and B denote the self-interstitial, vacancy, silicon lattice site and boron, respectively.

The objective of this thesis is to expand the model of Sinno (1998) by accounting explicitly for the formation of boron complexes by reactions with interstitials and vacancies. Conservation equations for each boron defect species were developed using thermophysical data obtained from electronic structure calculations (Rasband and Clancy, 1996; Luo, Rasband and Clancy, 1998). The model is parametrized using the experimental OSF-Ring data of Dornberger et al. (1997) which relates the position of the OSF-Ring to the doping concentration of boron in the melt. The results are used to postulate a mechanism for boron-mediated OSF-Ring dynamics.

OSF-Ring dynamics is set by point defect and impurity dynamics within a narrow region near the melt-crystal interface. The effects of boron on IV dynamics can be understood qualitatively from reactions (1)-(6). Near the melt-crystal interface the complexes BI and B_2I store interstitials temporarily and dampen depletion of interstitials caused by IV recombination. Then, interstitials are released by the dissolution of BI and B_2I yielding higher interstitial concentrations. All of these processes occur in the region where the self-interstitial and vacancy balance is still evolving. These observations lead to the conclusion that the kick-out reaction is fast enough to consume interstitials quickly and release them back within a short axial distance to achieve lower effective interstitial diffusion and to shift the OSF-Ring inward. This phenomenon is known as the chemical pumping mechanism (Hu, S.M., 1994) and is observed in both interstitial and vacancy release mechanisms of BI, B_2I and BV. These boron complexes can therefore act as traps which slow intrinsic point defect diffusion. This also means that the kick-out mechanism is assumed to be dominant and is the cause of on the OSF-Ring shift at high boron concentrations. Our extension of the microdefect model includes boron point defect chemistry described in Equations (2) to (6). The extended model is able to predict the experimental observations with only adjustment of binding entropies.

Thesis Supervisor: Robert A. Brown

Title: Provost of MIT and Warren K. Lewis Professor of Chemical Engineering

Acknowledgements

Thanks be to God for my graduate study life and all things that work together for good. My sincere thanks to my research advisor, Prof. Robert A. Brown, who played a major role in my scholastic and professional development, for his continuous support on this project, making the road to an Engineer degree possible. I would like to express my gratitude to Dr. Talid Sinno for his patience, truly invaluable comments and critical reading of the manuscript. I gratefully acknowledge the financial support by the Consortium on Defect Dynamics in Silicon at MIT, Office of Naval Research and Prof. Brown. Thanks to Prof. Robert E. Cohen for being the greatest motivator in the department giving me the opportunity to walk alone for the last Engineer degree. To Ms. Wei Wei Luo from Chemical Engineering Department at Cornell University for her valuable and patient discussions on the energetics of boron complexes. Going back in time, I am still sincerely grateful to Prof. Scriven and Dr. Ian Gates at the University of Minnesota for all the learning experience that I had.

Thanks to my friends in the department whose continuous support realized the sense of being together in my MIT experience, to Chandrasekar Papudesu for all your advice, support and confidence in me, to Neeraj Sangar for the stimulating late night sharing, inputs and discussions, and to Betty Yu for accompanying me in all activities that made my MIT experience a well-balance and colorful graduate student life at MIT.

To my best friend and beloved brother, Christopher Lembong, my greatest thanks for everything he has done in my life and for assuring that he is with me, as we trust God in times of joy and difficulty. I adore being your best friend, Chris, and as you are rejoicing in heaven, our faithful friendship is carved in my life and my ministry, and I will delight in the Lord, trust in Him and make my whole life as the best sacrifice for Him. Sincere thanks to Hanny Setiawan for teaching me to improve the music of my life, strengthening me in faith and the special joy of just being together. Thanks to Glory Hardjadinata for assuring me that Christianity does exist and God is good, therefore, all my problems and difficulties did not look so bad. Thanks to my dear cousin, Wendy Surya who gave me support and confidence to do all the best for God with His gifts. Thanks to Airin Adianto for simply checking in, giving a tea cup of encouragement, and reminding

me to hold on to child life faith, to be strong, and to stand firm in God. To my brothers and sisters in the Indonesian Christian Fellowship-Boston and the Christian Pentecostal Church-Newton, thank you for the wonderful time, prayers and fellowship, you all are also mean a lot to me.

I would like to thank my parents for my invaluable education and to dedicate this thesis to my parents and Chris. Without their encouragement, I am not what I am and I thank them for loving me as who I was, who I am and who I would be. To my mom Yany Herawati, for your continuous prayers for me and reminding me to simply always give thanks to the Lord in all circumstances. To my dad Jemy Susanto, for encouraging me to do the best and not worry about being the best and trusts his son wholeheartedly. To my lovely sister Yeli Astrea Susanto, thanks for your continuous support and prayers, I am as proud of as you are proud of me. To my dearest brothers Edwin Susanto and Andi Susanto, I am grateful for the loving heart care of you. Thanks are also given to my lovely aunt Aminah, without whom I would not be what I am right now and you do not realize how great your contribution is in my childhood and my life.

Finally, from my heart, I am grateful to God for all of you, the dear people in my life ... you know exactly who you are ... for your spoken or written words that have continually flooded my heart with a sea of loving support. When I am troubled, I can look at the sky and smile. Even though you live a long way away and do not know my struggle, it is enough to just simply remember that I am loved and you are there always praying for me. It lifts my spirit, unfailingly turns my attitude from surly to sunny, revives a milieu of memories, and makes me thank the Lord endlessly for all of you in my life.

As I look back over my years in MIT, God has surely been most faithful and He is so much more than kind. Though I might not have enough sleep, by His grace God blessed me abundantly more than dreams could ever be. Finally, I did graduate with an Engineer degree from MIT, praise God! "And we know that all things work together for good to them that love God, to them who are the called according to His purpose" (Roman 8:28).

In thankfulness to my faithful God, I love my life and with all my heart, soul and strength, I love my God, Jesus Christ.

Contents

List of Figures

List of Tables

1. Introduction

1.1 Introduction and Background

As silicon-based microelectronic devices become increasingly complex, two main challenges are encountered within the silicon wafer industry. The first is the production of very large diameter (≥ 300 mm) wafers to accommodate the increasing size of microelectronic devices. The second is the reduction of microdefect concentration and size to allow for acceptable device reliability as linewidths shrink past the 1 μm length scale. The silicon wafer industry today relies on the Czochralski method for growing the single crystal silicon used to fabricate these devices.

In the Czochralski growth process, a seed crystal with the desired crystallographic orientation is contacted with silicon melt that is contained in a heated crucible. The Czochralski growth begins by establishing dislocation free growth within the neck portion of the crystal. The crystal diameter is then allowed to increase to the desired size by adjusting the heated power within the Czochralski system. A crucial component of silicon crystal growth is doping, which refers to the controlled addition of certain impurities to the melt in order to produce crystals with certain electrical properties; examples of such dopants are Boron, Arsenic, Phosphorus (Fahey, 1989). In the Czochralski process, the crucible and the crystal are usually counter-rotated to produce uniform dopant distribution within the crystal. Once the crystal ingot is grown, it is sliced into wafers which are then chemically and mechanically polished to yield a substrate for microelectronic device fabrication.

The control of microdefects during crystal growth has been the focus of numerous studies for many years. It is well known that the primary constituents of these microdefects are intrinsic point defects, namely self-interstitials and vacancies. The composition and size of the microdefects are a strong function of the thermal history and operating conditions within the crystal growth system during growth. These relationships have been probed in detail with numerical simulations of the heat transfer environment and point defect dynamics (Sinno, 1998).

The presence of dopants and other impurities further complicates the observed microdefect distribution. It is very likely that these impurities affect microdefect distributions by interacting

directly with self-interstitials and vacancies. The goal of this thesis is to characterize these interactions using numerical simulation of point defect dynamics during Czochralski silicon crystal growth.

1.2 The Oxidation-Induced Stacking-Fault Ring

The focus of the simulations is the so-called Oxidation Induced Stacking Fault Ring (OSF-Ring). The OSF-Ring is a neutral region where the concentrations of self-interstitials and vacancies are essentially in balance. A large portion of the modeling and simulation of point defect dynamics have been aimed at predicting the behavior of the OSF-Ring with respect to the crystal growth operating conditions. These efforts have been motivated by the apparent simplicity of the OSF-Ring dynamics with changes in pull rate and temperature field.

The OSF-Ring separates regions of vacancy rich and interstitial rich defects and divides the crystal into a poor gate oxide quality area inside the OSF-Ring from an excellent gate oxide quality area outside the ring (Sinno, 1998). The OSF-Ring has been studied extensively under different pulling conditions for low boron dopant concentrations of less than 10^{17} cm^{-3}. The OSF-Ring diameter has been determined to be a function of the temperature gradient at the solid melt interface and the pull rate. The OSF-Ring shifts outward when the pull rate is increased. Conversely, a low pull rate allows interstitials to diffuse radially inward and the OSF-Ring is shifted inward as a result. The smaller the axial temperature gradient, the more sensitive the OSF-Ring diameter is to changes in pull rate.

The dynamics of the OSF-Ring can be explained, both quantitatively and qualitatively, in terms of the dynamics of native point defects, vacancies and the self-interstitials. In the cold upper portion of the crystal where point defect concentrations are frozen, it is convenient to define a quantity Δ which represents the difference in concentrations between interstitials and vacancies (Voronkov, 1982),

$$\Delta(R,Z) \equiv C_I(R,Z) - C_V(R,Z). \tag{1.1}$$

A positive value for delta indicates that self-interstitials are in excess while a negative delta indicates vacancies are in excess. Inside the OSF-Ring, vacancy related defects such as Flow

Pattern Defects (FPD) and Crystal Originated Particles(COP) are formed, while interstitial related defects are found outside the ring (Yamagishi et al., 1992). Illustration of the radial point defect field surround the OSF-Ring is shown in Figure 1-1. Sinno (1998) has proposed a model for interstitial and vacancy (IV model) dynamics to predict OSF-Ring dynamics without impurities. The position of the OSF-Ring was predicted by the condition $\Delta(R_{OSF}, Z) = 0$ at the top of crystal and was shown to depend on the crystal growth conditions, measured by the pull rate and the temperature field in the crystal.

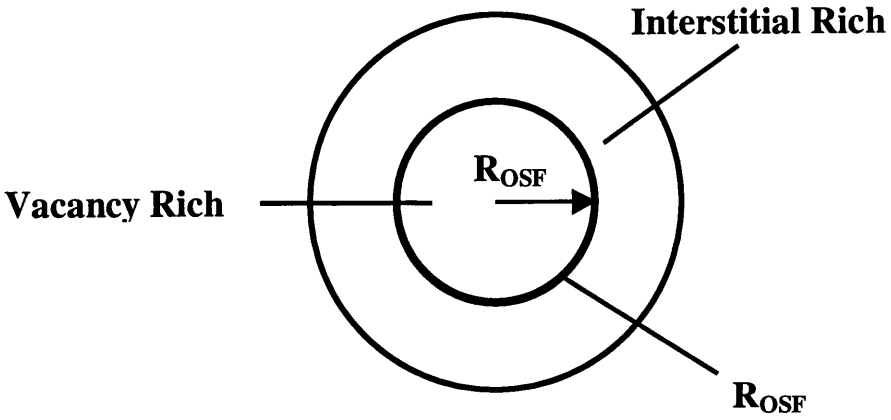

Figure 1.1

Radial point defect field surrounding the OSF-Ring.

At high pull rates, the OSF-Ring is located at the crystal surface. When the pull rate is decreased, there is more time for interstitials to diffuse inward, therefore, the OSF-Ring diameter shrinks until it disappears in the wafer center at a critical pull rate (V_{crit}), which depends on the axial temperature gradient. The OSF-Ring position is correlated simply to the ratio of the pull rate (V) and the axial temperature gradient (G) at the melt-crystal interface at the corresponding OSF-Ring radius, $R=R_{OSF}$ according to the simple empirical relationship (von Ammon et al., 1995),

$$\left(\frac{V}{G_{(R_{OSF})}}\right)_{crit} \approx 1.34\text{x}10^{-3}\ \text{cm}^2/\text{min K}. \qquad (1.2)$$

A detailed asymptotic analysis of the point defect concentration profiles in the region near the melt-crystal interface has been performed by Sinno (1998), which explains the origin of this correlation. The analysis is discussed further in Section 3.2 in the context of the evolution of the boron complex concentration profiles.

1.3 OSF-Ring Dynamics with Boron Doping

The radius of the OSF-Ring has been shown to depend sensitively on the boron concentration above the threshold value of $3x10^{18}$ cm^{-3} (Dornberger et. al, 1997). At low dopant levels, the OSF-Ring position depends exclusively on the operating growth conditions and is independent of boron concentration. However, growth experiments by Dornberger et al. (1997) have shown that addition of high boron dopant concentrations ($1x10^{15}$ - $2x10^{19}$ cm^{-3}) shifts the OSF-Ring toward the center of the crystal without changes in the crystal growth conditions. The effect of boron on the OSF-Ring position concentration is shown in Figure 1-2 for a 150 mm crystal. The accuracy of the experiments is about ± 5 mm for the ring measurements and 5% in the boron concentration (Dornberger E., 1998).

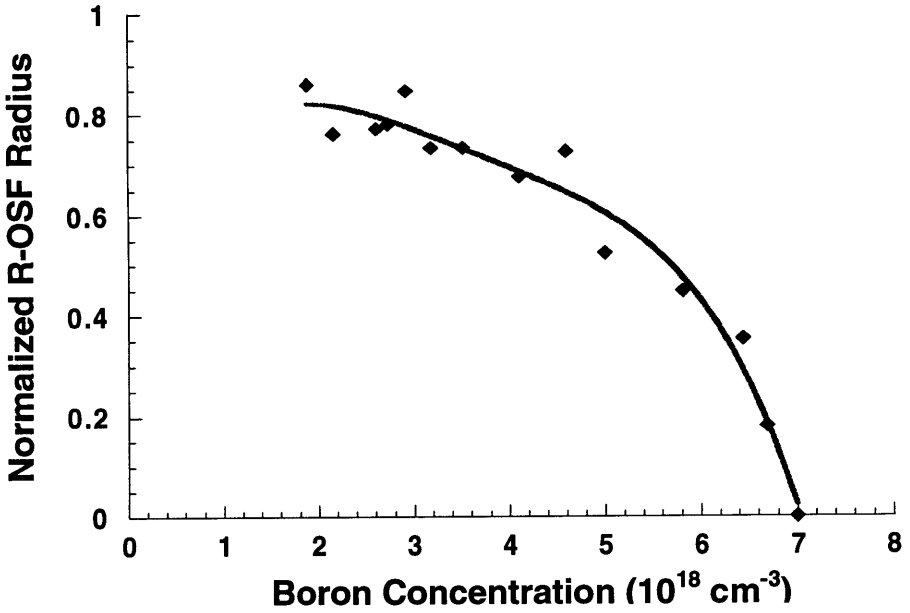

Figure 1-2

Observed OSF-Ring dynamics for various boron doping levels (Dornberger et al., 1997).

These experimental results suggest that boron doping has an effect on intrinsic point defect concentrations. Furthermore, it is well known that the OSF-Ring position is set in a region close to the melt-crystal interface where crystal temperature is high (Sinno, 1998). In order for boron to

affect OSF-Ring dynamics, we expect boron-point defect interactions to occur in this region. In general, a shrinking of the OSF-Ring diameter is the result of a shift of the point defect balance in favor of self-interstitials, either by vacancy depletion or self-interstitial addition. Interactions of intrinsic point defects with boron atoms may result in a reduction of vacancies and/or an increase in interstitial concentration near the melt-crystal interface of the growing crystal. The goal of this research has been to couple a model for the solid-state chemistry of boron in silicon with the model for the dynamics of native point defects in order to predict the shift in the OSF-Ring with boron concentration.

1.4 Objectives

The dynamics of the OSF-Ring have been explained quantitatively for crystals containing only self-interstitials and vacancies (Sinno, 1998). The model of Sinno (1998) was based on the solution of two coupled partial differential equations describing the distribution of interstitial and vacancy within the growing crystal under a specified thermal field. The goal of this thesis is to expand this model by accounting explicitly for the formation of boron complexes by reactions with interstitials and vacancies. Conservation equations for each boron defect were developed using thermophysical data obtained from electronic structure calculations (Rasband and Clancy, 1996; Luo, Rasband and Clancy, 1998). The model was parametrized using the experimental OSF-Ring data of Dornberger et al. (1997) which relates the position of the OSF-Ring to the doping concentration of boron in the crystal. The results are used to postulate a mechanism for boron-mediated OSF-Ring dynamics.

2. Model for Boron Defect Dynamics

2.1 Model for Intrinsic Point Defect Dynamics

The point defect dynamics model described by Sinno (1998) for the Czochralski silicon growth consists of point defect transport by Fickian diffusion and bulk crystal motion, and the consumption or generation of point defects by recombination. The above processes are described mathematically by

$$\nabla \cdot \left(-D_i(T)\nabla C_i\right) + V\frac{\partial C_i}{\partial z} + R_i = 0, \qquad (2.1)$$

where the subscript i=I,V represents the point defect species, D_i is the diffusion coefficient, V is the axial pull rate, C_i is the concentration in atom per unit volume (cm^{-3}), and R_i represents any related solid state reaction. The diffusion rates and the rates of solid-state species reactions determine the differences in the self-interstitial and vacancy concentrations at a given temperature and thus set the value of $\Delta(R,Z)$ in Equation (1.1).

2.2 Boron Transport and Chemistry

2.2.1 Chemistry of Boron in Silicon

Group III elements and group V elements are common dopants in Silicon (Fahey, 1989). When a dopant is present, the intrinsic defect concentrations in the crystal are either increased or decreased. Boron is universally used as a p-type dopant in the fabrication of silicon devices but the mechanism for boron diffusion is not yet completely understood. Many experiments and studies have shown that boron diffusion in silicon is dominated by an interstitial mechanism. At high boron

concentrations, boron dopant clusters become important, especially in the presence of a large excess of self-interstitials that lead to a large number of mobile boron atoms (Zhu, 1996).

In this thesis, the previous intrinsic point defect dynamics model of Sinno (1998) is extended to include boron-point defect interactions in the crystal. The following reactions are considered:

$$I + V \leftrightarrow 0, \tag{2.2}$$

$$B + B \leftrightarrow B_2, \tag{2.3}$$

$$B + I \leftrightarrow BI, \tag{2.4}$$

$$B_2 + I \leftrightarrow B_2I, \tag{2.5}$$

$$B + V \leftrightarrow BV, \tag{2.6}$$

$$BI + V \leftrightarrow B. \tag{2.7}$$

The Frenkel pair IV generation/recombination reaction (Equation 2.2) is defined as the removal of an atom from a lattice site, followed by its transfer to an interstitial site, where I, V, 0 denotes the self-interstitial, vacancy and silicon lattice site respectively. Recombination was included in Sinno's model of point defect dynamics (1998).

In this work, boron (B) is assumed to reside in the substitutional site in which a boron atom resides on a silicon lattice site (Zhu, 1996). We consider the formation of B_2 clusters (Equation 2.3) only, as larger boron clusters are relatively unstable (Luo, Rasband and Clancy, 1998). Reactions of boron with intrinsic point defects lead to the formation of boron-interstitial (BI) and boron-vacancy (BV) pairs, as shown in Equations (2.4) and (2.6), respectively. The B_2 clusters are assumed to interact only with interstitials to form B_2I (Equation 2.5) as other species have been found to be unstable (Luo, Rasband, Clancy , 1998). The dissolution of a BI defect by reaction with a vacancy (Equation 2.7) is known as the Frank Turnbull reaction (Frank and Turnbull, 1956) and also has been shown experimentally to be an energetically favorable reaction. Equations (2.3), (2.6) and (2.7) are mainly responsible for boron diffusion within the silicon lattice and are discussed in more detail in Section 2.2.2.

A significant limitation to modeling microdefect formation quantitatively is that, experimentally, it is difficult to measure the exact concentrations of most defect species. In silicon, point defects are present in very low concentrations and it is still difficult to directly study defect interactions and obtain accurate microscopic defect parameters such as diffusivities and equilibrium

concentrations. The diffusion coefficients of both intrinsic point defects and boron complexes together with the mechanism of boron-point defect interactions are still not well understood. Estimates for equilibrium coefficients of boron complexes used in this thesis were inferred from the results of Empirical Tight Binding (ETB) atomistic simulation and the Stillinger-Weber interatomic potential based on recent studies of the interactions between boron and intrinsic point defects in silicon (Rasband and Clancy, 1996; Luo, Rasband and Clancy, 1998). These thermal equilibrium concentrations of boron related defects were calculated as functions of binding enthalpies, binding entropies, and temperatures.

2.2.2 Mechanisms for Boron Diffusion

In silicon, dopants reside almost entirely on substitutional lattice sites. Substitutional dopant atoms are known to be immobile and atomistic interactions between native point defects and dopants are crucial for dopant diffusion because the dopant must interact with native point defects (vacancies and interstitials) to move from a lattice site to another.

An interstitial can displace a substitutional dopant into an interstitial configuration by the reaction sequence

$$B + I \leftrightarrow BI, \qquad (2.8)$$

$$B + I \leftrightarrow B_I. \qquad (2.9).$$

Equations (2.8) and (2.9) are known as the "kick-out" mechanism. In the first reaction (Equation 2.8) a boron atom in a substitutional site is kicked out by an interstitial to form a boron-interstitial pair (BI), whereas in the second reaction (Equation 2.9) a boron atom residing on an interstitial position (B_I) is produced instead.

Recently, Zhu (1996) found that there are three possible configurations formed by a boron atom and a Si interstitial; the boron-interstitial, which is formed by interstitial an interstitial silicon atom "kicking-out" the substitutional boron atom, a substitutional boron atom with a Si interstitial close by, and the B-Si interstitialcy (one boron and one Si atom sharing one single site). The second type was found to possess the lowest energy (Zhu, 1996). The interstitial and interstitialcy mechanisms may proceed simultaneously; for example, a silicon interstitialcy may kick a

substitutional dopant atom into an interstitial position, or a silicon interstitial may force a substitutional dopant atom into an interstitialcy configuration (Fahey, 1989).

At this point there is no clear distinction between interstitial boron and a boron-interstitial pair. Fahey (1989) has stated that it is difficult to distinguish experimentally between the two. Luckily, the distinction between the dopant interstitial and interstitiacy mechanisms may not be important from physical considerations and numerical evaluation. Both kick-out mechanisms for interstitial mediated diffusion give rise to the same diffusion equations and are completely equivalent (Chao, 1996). In the reverse directions, both reactions involve interstitials and the boron atom returns to a substitutional site.

Ab initio pseudopotential studies of diffusion and pairing processes in crystalline silicon have shown that the migration energy of the kick out reaction is about 1.0 eV and the energy barrier for the reverse kick-out in the absence of vacancies is 0.6 eV, which is much higher than the boron-interstitial migrational barrier (0.3 eV). This higher reverse kick-out reaction barrier allows the B interstitial to diffuse some characteristic distance before returning to a substitutional site (Zhu, 1996). Boron diffusion is enhanced through this kick-out mechanism. This also is supported experimentally because the migration barrier for boron diffusion in silicon is significantly lowered in the presence of excess interstitials.

In the Frank Turnbull mechanism, the interchange involves a vacancy that recombines with the boron-interstitial species and yields a boron atom on a substitutional site:

$$BI + V \leftrightarrow B. \qquad (2.10)$$

Here, the boron dopant atom B is in a substitutional site and BV is the boron-vacancy pair. The Frank Turnbull reaction is known to enhance or retard the dopant diffusion depending on the vacancy concentration (Frank and Turnbull, 1956).

Dopant atoms diffuse in pairs, either by an interstitial mechanism, a vacancy mechanism, or both in the forms of a dopant vacancy pair, a dopant interstitial pair or a dopant interstitialcy pair. Experimental evidence indicates that the interstitial mechanism dominates for p-type dopants, while the vacancy mechanism dominates for n-type dopants (Fahey, 1989). Some recent experiments concluded that the presence of excess interstitials greatly reduces the migration energy barrier for boron and therefore enhances boron diffusion rates; therefore boron diffusion is mediated predominantly by interstitials. The experimental results of Gossmann et al.(1997) and Tan and Gosele (1985) have shown that fractional interstitialcy diffusion component of boron is close to

unity. Enhanced boron diffusion also was observed by Fair (1975), Uematsu (1997) and Fahey et al. (1987).

With the above mechanisms, a substitutional boron atom can move from one lattice site to another either by the interstitial or vacancy assisted diffusion before it goes back to the substitutional state. This process is called mechanism of boron diffusion.

2.2.2 Estimates for Boron Diffusivity

Diffusion is one of many processes characterized by an energy barrier between the initial and the final states and the magnitude of this barrier is called the activation energy of the process (Kingery, 1976). As the temperature is increased, the number of atoms having sufficient energy to surpass this barrier increases exponentially, so that the temperature dependence of diffusion is represented as

$$D_i = D_o \exp\left(\frac{-E_a}{k_B T}\right) \tag{2.11}$$

in which D_i is the diffusion coefficient of species i, D_o is the pre-exponential factor and E_a is the apparent energy barrier for diffusion. Diffusion coefficients are very sensitive to the energy barrier.

Despite a good understanding of dopant diffusion at low concentration, dopant diffusion at high concentrations is not well understood. Both native point defects and boron complexes exist in several charge states depending on the dopants considered. Diffusivities of boron clusters are expected to be much lower than defects involving only one boron atom (Vandenbossche and Baccus, 1993).

Data from several studies of boron diffusion are shown in Table 2-1 along with the magnitudes of the diffusivity predicted at the melting temperature. Interstitial and vacancy diffusivities are taken from Sinno (1998). Several diffusivity estimates for boron and boron complexes (B, BI and BV) from different literature sources also are tabulated. Average values of the diffusivities were calculated and used in the model for boron defect dynamics.

The results of Mathiot and Pfister(1984) were obtained by fitting experimental measurement of boron profiles in an inert ambient in the temperature range 850-1100 °C. The

boron-pair cluster of interest B_2, is assumed to be immobile with zero diffusivity. In addition, boron clusters are assumed to be immobile as is B_2I. The calculated binding energy of BV (0.5 eV) is smaller than its estimated migration energy (1 eV) so the BV pair is not a stable diffusing species (Nichols et al, 1989).

Table 2-1

Diffusivity parameters for intrinsic point defects and boron complexes.

Defect of Interest	D_o (cm^2/s)	E_a (eV)	$D_i(Tm)$ (cm^2/s)	Source
I	0.242	0.937	$3.79x10^{-4}$	Sinno, 1998
V	10^{-3}	0.437	$4.28x10^{-5}$	Sinno, 1998
B	0.76	3.46	$3.33x10^{-11}$	Wolf and Tauber, 1986
	2.64	3.60	$4.41x10^{-11}$	Mathiot and Pfister, 1984
	1.0	3.5	$3.33x10^{-11}$	Orr Arienzo et al., 1988
	3.17	3.59	$3.33x10^{-11}$	Fair, 1975
	1.89	*3.54*	*$4.86x10^{-11}$*	*Average*
BI	$1.44x10^{-2}$	2.53	$3.84x10^{-10}$	Vandenbossche and Baccus, 1993
	$5.2x10^{-2}$	2.31	$6.32x10^{-9}$	Mathiod and Pfister, 1984
	$3.32x10^{-2}$	*2.42*	*$1.90x10^{-9}$*	*Average*
BV	$4.00x10^{-6}$	1.28	$5.89x10^{-10}$	Mathiot and Pfister, 1984

2.2.3 Equilibrium Property Estimates for Boron Complexes

The point defect reactions are driven by the relative supersaturation of the individual defect species. The supersaturation of each point defect species is directly related to its local equilibrium concentration. We estimated equilibrium concentrations by using a combination of atomistic simulation and fitting to OSF-Ring dynamics data. Equilibrium concentrations of vacancies and self-interstitials are given by:

$$C_I^{eq}(T) = 2.97\,10^{23}\exp\left(\frac{1.40+3.85\text{x}10^{-3}T}{k_B}\right)\exp\left(-\frac{3.46+3.08\text{x}10^{-4}T}{k_B T}\right) \qquad (2.12)$$

$$C_V^{eq}(T) = 4.97\,10^{22}\exp\left(\frac{-3.70+3.53\text{x}10^{-3}T}{k_B}\right)\exp\left(-\frac{2.48+2.33\text{x}10^{-4}T}{k_B T}\right) \qquad (2.13)$$

where C_I^{eq} and C_V^{eq} represent the thermal equilibrium concentration of interstitials and vacancies (Sinno, 1998). Equilibrium concentrations for substitutional boron can be related to the solid solubility limit of boron in silicon in the range of 900-1325°C (Armigliato et al., 1977):

$$C_B^{eq} = 9.25\text{x}10^{22}\exp\left(\frac{-0.73\,\text{eV}}{k_B T}\right)\text{cm}^{-3}, \qquad (2.14)$$

which is about $1\text{x}10^{20}$atom/cm^{-3} at 1683 °K.

We assume that the formation of each of these boron complexes involves a substitutional boron atom rather than an interstitial one. This is a good assumption given that the substitutional state is much more stable and most of the free boron in a silicon lattice is substitutional (Zhu, 1996).

Equilibrium concentrations for defects involving boron atoms were calculated based on Empirical Tight Binding simulations (Rasband and Clancy, 1996; Luo, Rasband and Clancy 1998). These calculations use a system containing 64 atoms (63 for a vacancy, 65 for an interstitial, etc). Using the perfect silicon lattice as a reference state, the equilibrium constant for the reaction which forms boron complex X, K^{eq}_X, is given by:

$$K_X^{eq} = \theta_X \exp\left\{\frac{S_X^f}{k_B}\right\} \exp\left\{-\frac{H_X^f}{k_B T}\right\}, \tag{2.15}$$

where θ_x is the orientational degeneracy which is a function of the geometrical configuration of the boron complex X, S^f_x and H^f_x are entropy and enthalpy of formation of X, respectively. Concentrations in the equilibrium constant shown in equation 2.15, are normalized to the concentration of lattice sites containing the defect, C_s, ($5x10^{22}$ cm^{-3} for silicon):

$$[X] = \frac{C_X}{C_s}. \tag{2.16}$$

Estimates for the formation energy of boron complexes were obtained from Empirical Tight Binding studies using two reference systems: the perfect silicon lattice and a silicon lattice with only one boron substitutional atom (Luo, Rasband and Clancy, 1998). The binding enthalpy and entropy of boron-interstitial clusters X are defined as:

$$E_X^b \equiv p E_I^f - E_X^f, \tag{2.17}$$

$$S_X^b \equiv S_X^f - p S_I^f, \tag{2.18}$$

where p is the number of interstitials in the cluster, E^b_X and E^b_X are the binding enthalpy and entropy, E^f_X and S^f_X are the formation enthalpy and entropy. The boron-vacancy cluster binding parameters are computed in a similar manner. Positive binding enthalpies and entropies are defined by the energy released and the entropy gained by each reaction. Values obtained using the Empirical Tight Binding method and static relaxation are calculated to within 0.2 eV uncertainty (Rasband and Clancy, 1996).

The equilibrium concentration for each defect species is estimated from the calculated binding energies and Equation (2.15). The equilibrium constant is expressed in terms of the binding energy as (see Appendix A for example)

$$K_X^{eq} = \theta_X \exp\left\{\frac{S_X^b}{k_B}\right\} \exp\left\{\frac{H_X^b}{k_B T}\right\}, \tag{2.19}$$

in which the K^{eq}_x for a specific defect was derived from the formation reaction.

Based on the studies discussed above, the boron kick-out mechanism is dominant and BI is believed to be important in our point defect model. Several values of the binding energy of BI cluster was reported in the literatures: 1.1 eV (Zhu et al., 1996), 0.6 eV (Mathiot and Pfister, 1984), 2.2 eV (Vandenbossche and Baccus, 1993), and 0.8 eV (Uematsu, 1997). The BV cluster is reported to be a stable species with binding energies estimated at 0.5 eV by Nichols et al. (1989) and 0.39 eV by Rasband et al. (1996b). Large substitutional boron clusters are unfavorable and the B_2 cluster is important when the boron doping level is above approximately 10^{18} cm^{-3} (Rasband and Clancy , 1996; Luo, Rasband, and Clancy, 1998). Furthermore, Empirical Tight Binding studies suggested that clusters containing two boron atoms occupying a substitutional site are stable, unlike other small boron clusters. The B_2I cluster is considered to be the most stable species among boron complexes, however, B_2 clusters involving vacancies are not energetically favored (Luo, Rasband and Clancy, 1998). We included B_2, BI, B_2I, and BV in their preferred charge states in the model for boron/point-defect chemistry.

Formation enthalpies and entropies for boron complexes based on Empirical Tight Binding calculations (Luo, Rasband, and Clancy, 1998) are listed in Table 2-2. The binding energies for boron complexes computed from Empirical Tight Binding calculations using static relaxation calculation (Rasband and Clancy, 1996; Luo, Rasband, and Clancy, 1998) and intrinsic point defect obtained from the parameter fitting of Sinno (1998) are listed in Table 2-3 (see Appendix B for calculations).

Table 2-2

Formation enthalpies and entropies of boron complexes

(Rasband and Clancy, 1996 and Luo, Rasband and Clancy, 1998).

Boron Complex	H^f_x (eV)	(S^f_x/k_B)	θ_x
B_2	-0.8	2.75	2
BI	3.1	1.9	4
B_2I	2.0	4.3	4
BV	2.3	3.3	4

Table 2-3

Binding energies of boron complexes.

Boron Complex	E^b(eV)	S^b/k_B
B_2	0.8	2.75
BI	0.87	-5.98
B_2I	1.17	-6.33
BV	0.85	1.06

2.2.4 Models for Boron Reaction Chemistry

Based on the diffusion limited reaction kinetics (Sinno, 1998), the rates of reaction for generation and consumption of the boron complexes are a function of the local equilibrium concentrations and reaction rate constant. Consequently, in a single reaction, each of the concentrations is expressed as a function of the equilibrium constant and other constituent local concentrations at equilibrium. Equilibrium concentrations of boron complexes were calculated from the results of Empirical Tight Binding Sand Stillinger Weber atomistic calculations (Rasband and Clancy, 1996; Luo, Rasband, and Clancy, 1998). The equilibrium constant and equilibrium concentration expression for boron complexes are listed in Tables 2-4 and 2-5. Based on the calculated binding energies and entropies, the thermal equilibrium concentration of boron-pair cluster (B_2) is about two order-of-magnitude higher than the solubility limit of boron. Table 2-6 lists the reaction expressions for boron-point defect interactions.

The rate coefficients for each reaction were estimated from diffusion-limited reaction theory and includes an activation barrier with both entropic and enthalpic contributions. This model for reaction kinetics gives temperature dependent rate coefficients for each reaction, as shown in Table 2.7. Here, k_{IV} is the reaction rate constant, a_r is the capture radius, π is the atomic volume, c_s is the atomic density of silicon, and ΔG_X is the free energy barrier against reaction. The sensitivity of our simulation results to this value is discussed in Chapter 3.

Table 2-4

Equilibrium constant and equilibrium concentration expressions of boron complexes.

Reaction	Equilibrium Constant	Equilibrium Concentration Expression
B_2 Formation	$K_{eq}^{B_2} = \frac{[B_2]}{[B]^2}$	$C_{B_2}^{eq} = \frac{C_B^{\,2}}{C_s}\theta_{B_2} \exp\left\{\frac{S_{B_2}^b}{k_B}\right\} \exp\left\{\frac{E_{B_2}^b}{k_B T}\right\}$
BI Formation	$K_{eq}^{BI} = \frac{[BI]}{[B][I]}$	$C_{BI}^{eq} = \frac{C_B C_I}{C_s}\theta_{BI} \exp\left\{\frac{S_{BI}^b}{k_B}\right\} \exp\left\{\frac{E_{BI}^b}{k_B T}\right\}$
B_2I Formation	$K_{eq}^{B_2I} = \frac{[B_2I]}{[B_2][I]}$	$C_{B_2I}^{eq} = \frac{C_{B_2} C_I}{C_s}\theta_{B_2I} \exp\left\{\frac{S_{B_2I}^b}{k_B}\right\} \exp\left\{\frac{E_{B_2I}^b}{k_B T}\right\}$
BV Formation	$K_{eq}^{BV} = \frac{[BV]}{[B][V]}$	$C_{BV}^{eq} = \frac{C_B C_V}{C_s}\theta_{BV} \exp\left\{\frac{S_{BV}^b}{k_B}\right\} \exp\left\{\frac{E_{BV}^b}{k_B T}\right\}$
Frank Turnbull	$K_{eq}^{BIV} = \frac{[B]}{[BI][V]}$	

Table 2-5

Reaction expressions of boron-point defect interactions.

Reaction	Reaction Expression
Frenkel Pair IV Recombination	$R_{IV} = k_{IV}\left(C_I C_V - C_I^{eq} C_V^{eq}\right)$
B_2 Formation	$R_{B_2} = k_{B_2}\left(C_B{}^2 - \frac{C_B^{eq\,2}}{C_{B_2}^{eq}} C_{B_2}\right) = k_{B_2}\left(C_B{}^2 - \frac{1}{\frac{K_{B_2}^{eq}}{C_s}} C_{B_2}\right)$
BI Formation	$R_{BI} = k_{BI}\left(C_B C_I - \frac{C_B^{eq} C_I^{eq}}{C_{BI}^{eq}} C_{BI}\right) = k_{BI}\left(C_B C_I - \frac{1}{\frac{K_{BI}^{eq}}{C_s}} C_{BI}\right)$
B_2I Formation	$R_{B_2I} = k_{B_2I}\left(C_{B_2} C_I - \frac{C_{B_2}^{eq} C_I^{eq}}{C_{B_2I}^{eq}} C_{B_2I}\right) = k_{B_2I}\left(C_{B_2} C_I - \frac{1}{\frac{K_{B_2I}^{eq}}{C_s}} C_{B_2I}\right)$
BV Formation	$R_{BV} = k_{BV}\left(C_B C_V - \frac{C_B^{eq} C_V^{eq}}{C_{BV}^{eq}} C_{BV}\right) = k_{BV}\left(C_B C_V - \frac{1}{\frac{K_{BV}^{eq}}{C_s}} C_{BV}\right)$
Frank Turnbull	$R_{BIV} = k_{BIV}\left(C_{BI} C_V - \frac{C_{BI}^{eq} C_V^{eq}}{C_B^{eq}} C_B\right)$

Table 2-6

Reaction rate constants of boron-point defect interactions.

Reaction	Reaction Rate Constant
Frenkel Pair IV Recombination	$k_{IV}(T) = \frac{4\pi a_r}{\Omega c_s}(D_I + D_V)\exp\left(-\frac{0.58 - T\left(2.29 + 7.38\text{x}10^{-3}\right)}{k_B T}\right)$
B_2 Formation	$k_{B_2}(T) = \frac{4\pi a_r}{\Omega c_s}(D_B + D_B)\exp\left(-\frac{\Delta G_{B_2}}{k_B T}\right)$
BI Formation	$k_{BI}(T) = \frac{4\pi a_r}{\Omega c_s}(D_B + D_I)\exp\left(-\frac{\Delta G_{BI}}{k_B T}\right)$
B_2I Formation	$k_{B_2I}(T) = \frac{4\pi a_r}{\Omega c_s}(D_{B_2} + D_I)\exp\left(-\frac{\Delta G_{B_2I}}{k_B T}\right)$
BV Formation	$k_{BV}(T) = \frac{4\pi a_r}{\Omega c_s}(D_B + D_V)\exp\left(-\frac{\Delta G_{BV}}{k_B T}\right)$
Frank Turnbull	$k_{BIV}(T) = \frac{4\pi a_r}{\Omega c_s}(D_{BI} + D_V)\exp\left(-\frac{\Delta G_{BIV}}{k_B T}\right)$

2.3 Simulation of Boron Defect Dynamics

2.3.1 Boundary Conditions

The point defect model in Equation (2-1) is solved with the following boundary conditions. Equilibrium conditions are imposed at the melt-crystal interface for the native defects (self-interstitials, vacancies, and for the boron defects, e.g. B and B_2). Since boron is introduced at high concentration, a significant amount of substitutional boron forms B_2. At the melt-crystal interface, it is assumed that the local equilibrium described by Equation (2.20) is already satisfied and the initial boron dopant concentration (C_B^o) introduced into the system consists of an equilibrium concentration mixture of B and B_2 ($C_{B(Z=0)}$ and $C_{B2(Z=0)}$) in Equation (2.21) as

$$\frac{K_{eq}^{B_2}}{C_s} \equiv \frac{C_{B_2(Z=0)}}{C_{B(Z=0)}^2}, \tag{2.20}$$

$$C_B^o \equiv C_{B_2(Z=0)} + C_{B(Z=0)}. \tag{2.21}$$

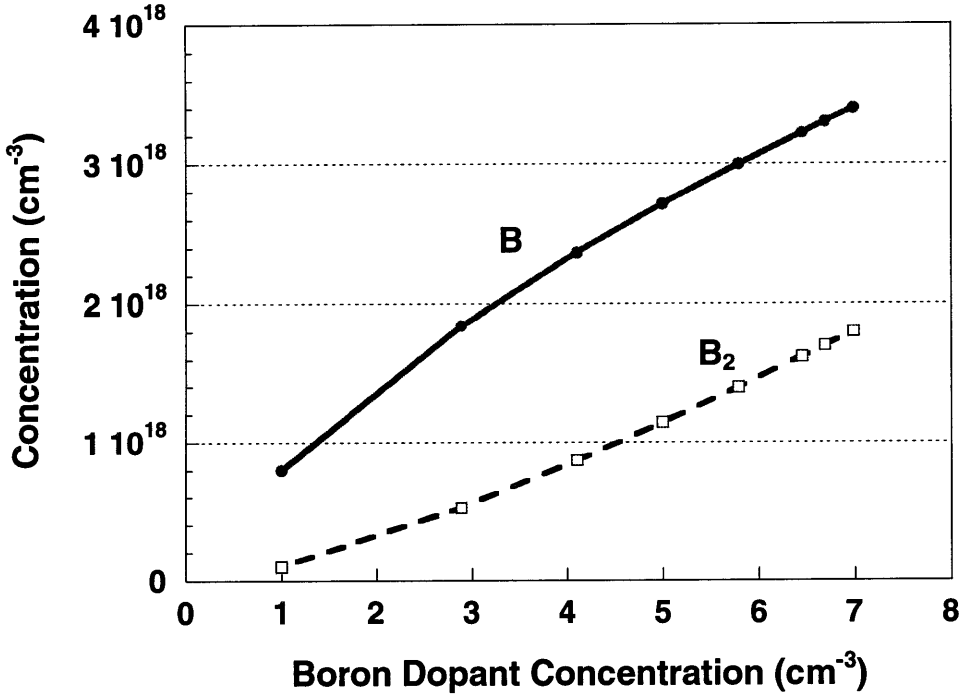

Figure 2-1

Boron (B) and boron pair (B_2) boundary conditions as a function of boron concentration.

Figure 2-1 shows that as the doping level of boron increases, a larger fraction of the boron is incorporated as B_2.

Boron complex concentrations (BI, B_2I, BV) are assumed to be zero at the melt-crystal interface. At the top of the crystal, zero flux conditions are imposed for all species. Zero flux conditions are also imposed for all species at the radial edge of the crystal, as described by Sinno (1998). The zero flux boundary condition represents a thin oxide layer formed by silicon-monoxide that evaporates from the melt (Dornberger et al., 1997)

2.3.2 Thermal Field and Crystal Geometry

Thermal field and crystal shape data was obtained from the heat transfer simulation of Dornberger et al. (1997b). We use an axisymmetric, two dimensional representation of the crystal in which the shape of the melt-crystal interface is fit to experimental measurements. All simulations described in Chapter 3 were performed using data computed for a 4" crystal grown at 1.7 mm/min. Note that the experimental OSF-Ring data described in Chapter 1 was not generated with the same conditions due to the unavailability of consistent data sets.

2.4 Numerical Method

The conservation equation (Equation 2.1) for all species and the boundary conditions represents a system of coupled, non-linear partial differential equations. This system of equations was discretized spatially using the Galerkin Finite Element Method (Sinno, 1998). The resulting system of algebraic system was solved using the Newton method. We employ zero-order continuation where all reaction rates are gradually increase from about 10^{-6} of their actual values. At each step, the solution from the previous solution is used as the initial guess for the next step. Upper bound diffusivities of B_2 and B_2I were assigned to the diffusivity of single boron atoms (B). Since single boron diffusivity is a few orders-of-magnitude smaller than the diffusivities of interstitial and vacancy, the effect of this assumption is negligible.

3. Results and Discussion

3.1 Comparison to Experimental Data

In order to allow quantitative evaluation of the models ability to fit the experimental data of Dornberger et al. (1997), polynomial fitting of the data in Figure 1.1 is performed. We used a fourth order polynomial fit to this data to give:

$$\text{R-OSF} = 0.41825 + 0.55617\, C_B - 0.25928\, C_B^2 + 0.047497\, C_B^3 - 0.0032805\, C_B^4. \qquad (3.1)$$

The simulation predictions are compared quantitatively to this curve by fitting the calculations to a n^{th}-order polynomial, where n is the number of simulation data points. The polynomial functions represented the experimental data and the simulation predictions are compared based on location, i.e.,

$$\chi = \frac{1}{n}\sqrt{\sum_{i=1}^{n}\left[R_{OSF}(C_{Bi}) - R_{OSF}^{exp}(C_{Bi})\right]^2}, \qquad (3.2)$$

where χ is a quantitative indication of the goodness of fit of the simulation predictions to experimental data.

3.1.1 Parameter Fitting

The objective function, χ in Equation (3.2) is minimized with respect to the thermophysical properties of the boron complexes. However, due to the large number of parameters, we choose a small subset for the optimization while keeping the others fixed. Our choice for the variable parameter subset is justified below, on the basis of sensitivity and uncertainty.

Sensitivity tests demonstrate that the simulation predictions are unresponsive to changes in the diffusion coefficients for the boron complexes. This is explained by noting that these

diffusivities are generally several order-of-magnitudes smaller than self-interstitial and vacancy rates. Thus, no diffusivities were used in the fitting. The activation barrier ΔG^B_X for all boron related reactions are arbitrarily assigned a value of 1 eV. This value is sufficiently small to give very large values for the Damkohler number (Da) for all reactions described by Equations (2.3) to (2.7), which compares the rate of reaction to the magnitude of the diffusion coefficients. The high Damkohler number limit established for reactions in (2.3) to (2.7) implies that all these reactions are transport limited and reach completion immediately for given local conditions. Physically unreasonable value for ΔG^B_X of several electron volts were required to establish Da ~ O(1) conditions. Activation barriers of less than 1 eV did not affect the simulation results in any way as the high Da limit had already been established for 1 eV. For this reason, ΔG^B_X is excluded from the fitting process and because of unavailability of any data, ΔG^B_X is excluded from further consideration.

The remaining properties are all associated with the equilibrium properties of boron related defect, i.e. the binding enthalpies and entropies. Simulation results are not very sensitive to either the pure boron cluster (B and B_2) energies or the boron-vacancy complex. The latter is not sufficiently stable to greatly affect the results and its binding energy and entropy are taken to be fixed.

Clancy et al. (1998) have computed all enthalpies using Empirical Tight Binding methods and we assume that those calculation are sufficiently accurate for all species. The entropies, however, are computed with the Stillinger-Weber potential and are subject to much larger uncertainty. We therefore use the binding entropies for the formation of BI and B_2I to fit our simulation predictions to the experimental data of Dornberger et. al. (1997) shown in Figure 1-1.

The fitting is performed by selecting a range of values for S^B_{B2I} and then minimizing the objective function χ, by adjusting S^B_{BI}. The combination of binding entropies that gave the lowest value of χ was selected as our 'best' fitting parameter set.

3.2 Results

The values for sets of the various binding enthalpies and entropies are shown below in Table 3-1 and illustrated in Figure 3-1. Fitting the binding entropies of BI and B_2I simply means distributing

the interstitial release mechanism between these two boron complexes in order to best reproduce the experimental data.

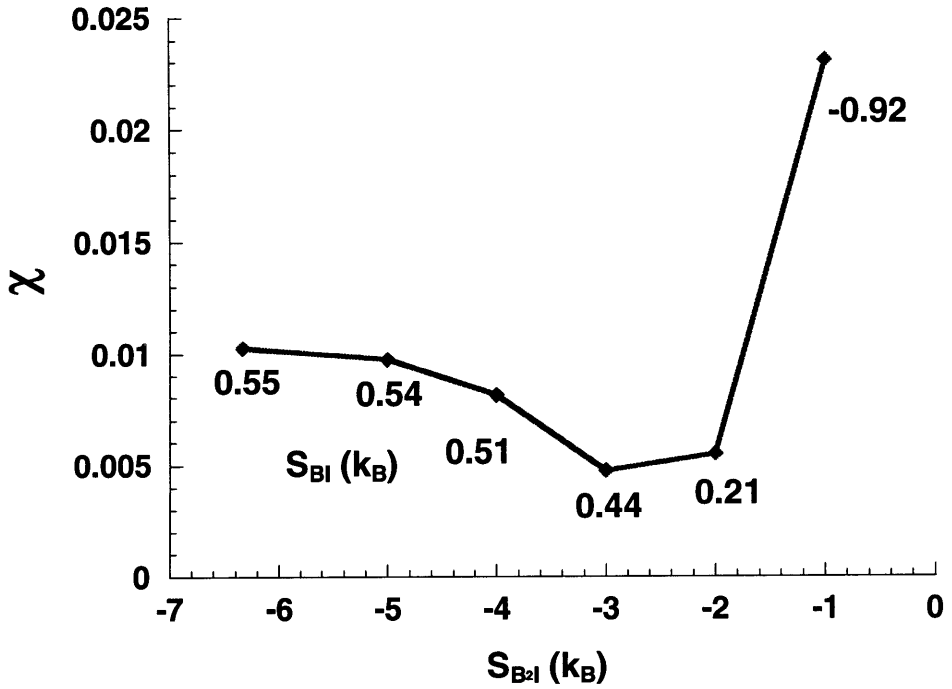

Figure 3-1

Global minimum of experimental for variation with S_{B2I}.

Table 3-1

Parameter sets used as best fit.

S^B_{B2I} (k_B)	S^B_{BI} (k_B)	χ
-6.33	0.55	10.25×10^{-3}
-5.00	0.54	9.73×10^{-3}
-4.00	0.51	8.13×10^{-3}
-3.00	0.44	4.76×10^{-3}
-2.00	0.21	5.51×10^{-3}
-1.00	-0.92	23.07×10^{-3}

By including all boron-point defect interactions, the microdefect model is capable of fitting the experimental data well. Our best results for this parameter set are shown in Figure 3.2 which swhos a comparison between the microdefect model prediction and the experimental data of Dornberger et al. (1997) for OSF-Ring position as a function of boron concentration.

The best microdefect parameters adjusted to reproduce the OSF-Ring curve are:

$H^b_{BI} = 0.88$ eV,

$S^b_{BI} = -0.44\ k_B$ adjusted from $S^b_{BI}{}^o = -5.98\ k_B$,

$H^b_{B2I} = 1.18$ eV unadjusted,

$S^b_{B2I} = -3.00\ k_B$ adjusted from $S^b_{B2I}{}^o = -6.33\ k_B$.

The agreement between the simulation results and the data of Dornberger et al. is good across a wide range of boron doping levels. The following sections provide insight into the mechanism that leads to the observed effect of boron doping on the dynamics of the OSF-Ring.

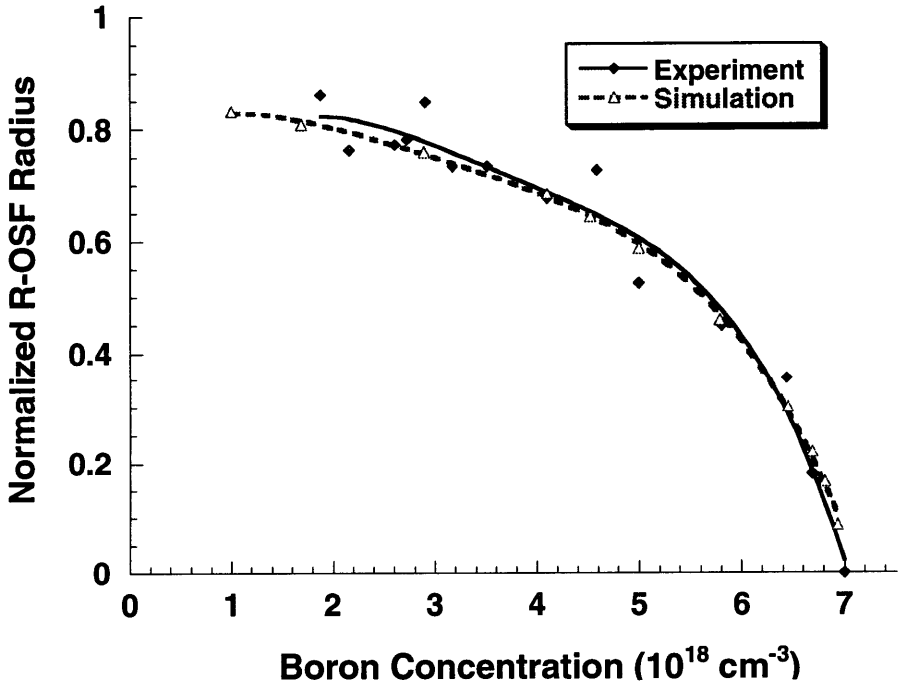

Figure 3-2

OSF-Ring radius as a function of boron concentration for experiment and simulation.

3.2 Mechanism for OSF-Ring Dynamics

Evolution of the $\Delta(R(Z),Z) = 0$ radial position occurs within a short axial distance from the melt-crystal interface. Initially, in the vacancy rich condition the $\Delta(R(Z),Z) = 0$ radial position is outside the perimeter and the farther from the melt-crystal interface, the more interstitials diffuse inward bringing the $\Delta(R(Z),Z) = 0$ radial position inward until it reaches a fixed position in the cold upper portion of the crystal. Figure 3.3 shows the $\Delta(R(Z),Z) = 0$ radial position along the axial direction from the previous IV Model (Sinno, 1998) and our extended model. Evolution of the self-interstitial and vacancy balance matters only for a short axial distance of one radius (Z^*/R).

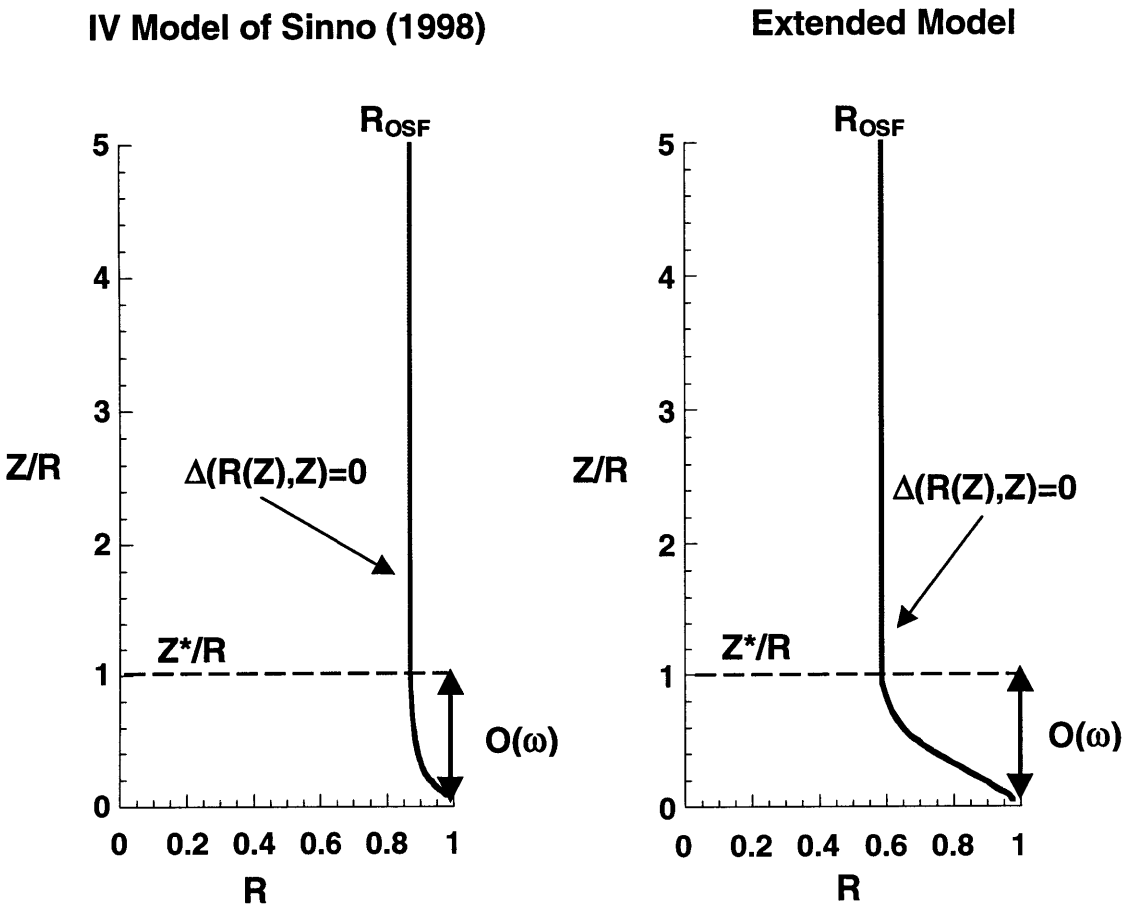

Figure 3-3

Evolution of the radial position of $\Delta(R(Z),Z) = 0$ along the axial direction from native point defect model of Sinno (1998) and the extended model with $5x10^{18}$ cm^{-3} boron.

The axial distance $O(\omega)$ over which the $\Delta(R(Z),Z) = 0$ condition continues to evolve has been determined using an asymptotic analysis of the coupled point defect conservation equations. Sinno (1998) have shown that ω is related to the magnitude of the characteristic activation energies contained in the diffusion and recombination coefficients. In the limit of high activation energies, these thermal activated processes decay very rapidly and confine point defect concentration evolution to a narrow region near the melt-crystal interface. For the operating conditions used to generate Figure 3-3, this distance is less than 1 radius in the axial direction. This distance is important when considering the effects of boron chemistry on native point defect concentrations. If reactions in Equation (2.3) to (2.7) occur slowly over length scales larger than $O(\omega)$, it is unlikely that any effect on the position of the OSF-Ring will be observed.

3.2.1 BI and B_2I

Counter intuitively, the boron-interstitial reaction increases interstitial concentration. In the vacancy rich region inside the OSF-Ring, IV recombination reaction leads to large excess of vacancies and therefore is interstitial limited. Both IV recombination and boron-interstitial formation compete for interstitial atoms. Under these conditions, IV recombination is restricted and fewer interstitials are depleted this way, instead some interstitials go to form boron-interstitial clusters. Once the interstitial concentration is sufficiently depleted, the boron-interstitial formation reaction proceeds in the reverse direction (dissociation reaction) releasing interstitials and boron atoms back to substitutional sites and subsequently results in higher interstitial concentration. Similarly, in the interstitial rich region, more interstitials and fewer vacancies were found compared to the previous IV model.

Both inside and outside the OSF-Ring, boron-interstitials are produced at an early stage near the melt solid interface. Starting from the melt-crystal interface, BI concentration rises up significantly. Still near the melt-crystal interface, boron-interstitials dissociate releasing interstitials before boron-interstitials gradually are formed again. In conclusion, boron-interstitials store interstitials temporarily and effectively dampen the depletion of interstitials causing a reduction in the rate of IV recombination. This behavior is illustrated more clearly in Figure 3-4 and 3-5, where

the IV superscripts denote the concentrations from model of Sinno (1998). At the region near the melt-crystal interface, boron-interstitials release interstitials giving higher interstitial concentration.

In the boron-point defect interactions, the boron-interstitial acts as temporary storage i.e. interstitials are stored in the slowly diffusing boron-interstitials. Therefore the diffusion of interstitials is inhibited by this mechanism which allows interstitial consumption to form boron-interstitials and then the boron-interstitials release the interstitial back. This interstitial release mechanism, also known as the chemical pumping of point defects (Hu, 1994).

In contrast to the BI interstitial release mechanism that always releases interstitials, the stability of B_2I determines whether the interstitial release mechanism effectively increases the interstitial concentration. At one extreme when the stability of B_2I is too high, the chemical pumping mechanism did not occur because interstitials were consumed in large amounts by B_2I formation then released in small amounts. Example of this situation is shown in Figure 3-6 which shows axial B_2I concentration profiles at different entropies values. At $S^b_{BI} = -3.00\ k_B$ the OSF ring position is inside. Here, increment in B_2I entropy value shifts the OSF-Ring inward until a certain point when it starts to shift the OSF-Ring out of the crystal instantly. At $S^b_{B2I} = 6.00\ k_B$ the OSF-Ring position is no longer inside the crystal. Interstitials are released near the melt-crystal interface by B_2I clusters. However, at high stability of B_2I, the amount of interstitials dissociated from both BI and B_2I is inadequate to compensate a great initial consumption of interstitials.

A comparison of axial concentration profiles of BI and B_2I shows that BI is more dominant in the interstitial release mechanism (Figure 3-7). Furthermore, the interstitial release mechanism of B_2I is not completely symmetric with the one of BI. This is due to the fact that boron at high concentration is forming B_2 while the evolution of OSF-Ring is still in progress. This is illustrated in Figure 3-8. Essentially, in the BI formation boron reactant and the interstitial are consumed by the IV recombination. Thus, the reaction is driven in the reverse direction to release more interstitials. Although interstitials are consumed by the IV recombination reaction, the B_2 is consumed faster to form B_2I. By *LeChatelier's Principle*, addition of B_2I reactant drives the reaction in the forward direction, thereby producing more B_2I. The reaction mechanisms for BI and B_2I are shown schematically in Figure 3-9.

The core of the kick-out mechanism is that the self-interstitials supplied cannot maintain the equilibrium concentration value because most of the self-interstitials are consumed to produce

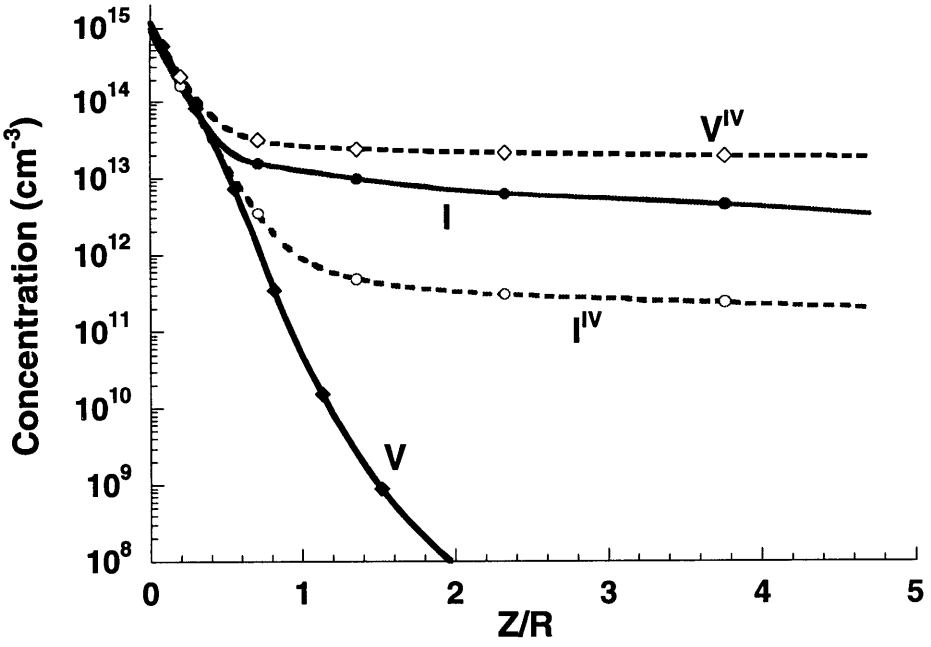

Figure 3-4

Axial concentration profiles of I and V at R=0.8.

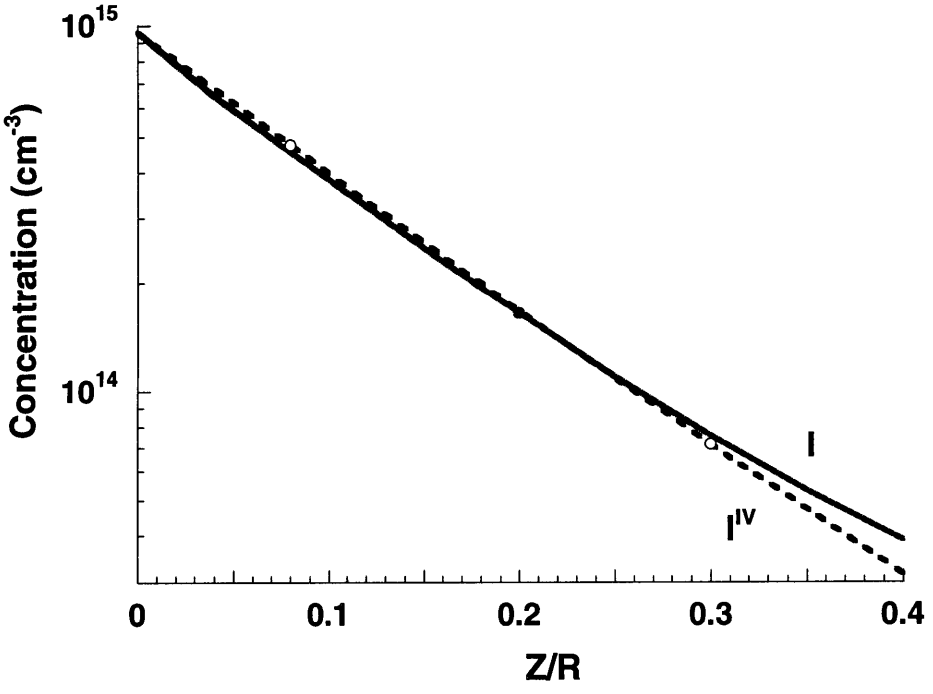

Figure 3-5

Axial concentration profile of interstitials near melt-crystal interface ($Z \leq 0.4$).

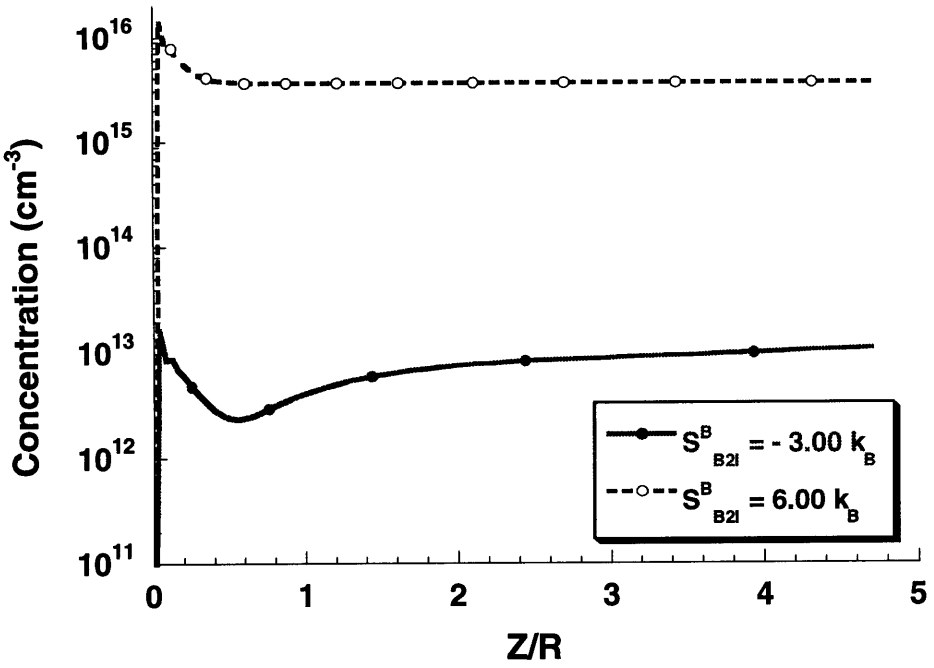

Figure 3-6

Stability of B_2I in the interstitial release mechanism.

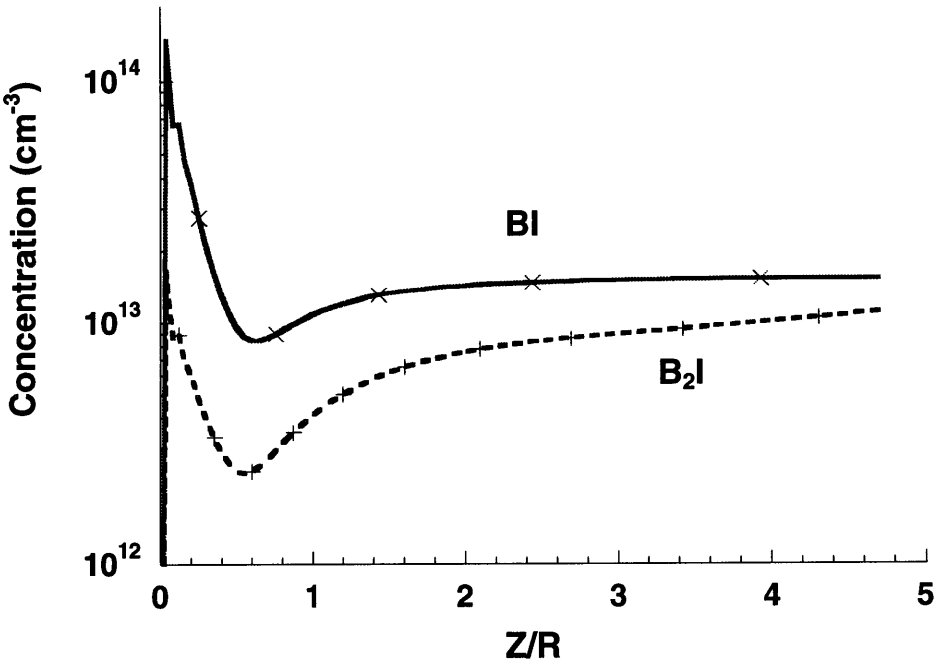

Figure 3-7

Axial concentration profiles of BI and B_2I complexes at R=0.8.

boron complexes by formation of BI and B_2I. Therefore, the reaction proceeds in reverse, returning the self-interstitials. All of these processes occur in the region where the evolution of the OSF ring is still dynamically moving and again it is within a radius distance ($Z^*/R = 1$). This is shown in Figure 3-10 and 3-11. These results lead to a conclusion that the kick-out reaction is fast enough to consume interstitials quickly and release them back within a radius distance to achieve lower interstitial diffusion and to shift the OSF-Ring inward.

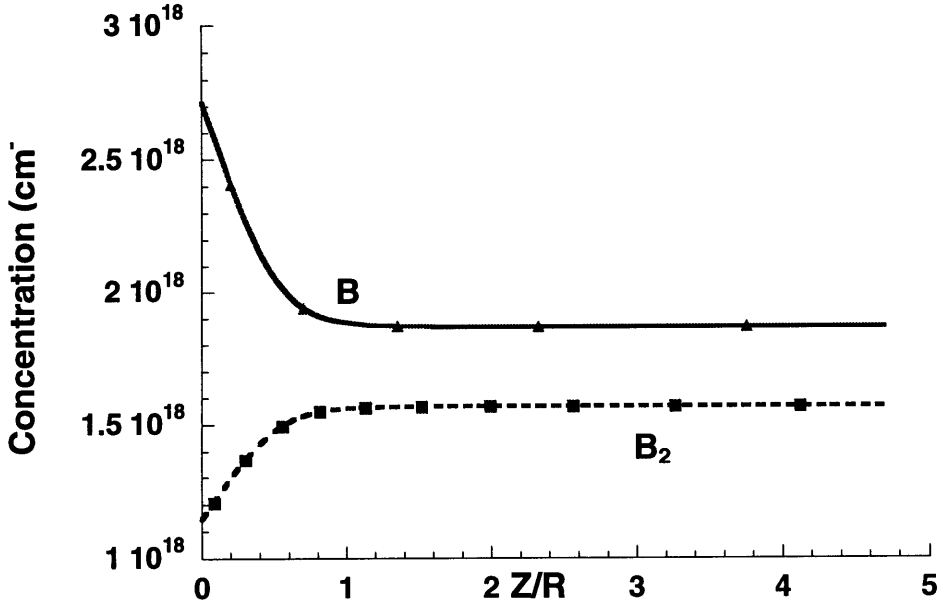

Figure 3-8

Axial concentration profiles of B and B_2 at R=0.8.

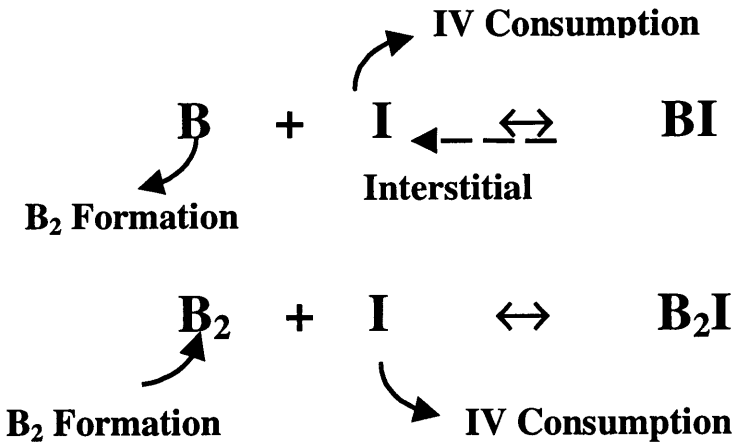

Figure 3-9

Reactant analysis of BI and B_2I formation.

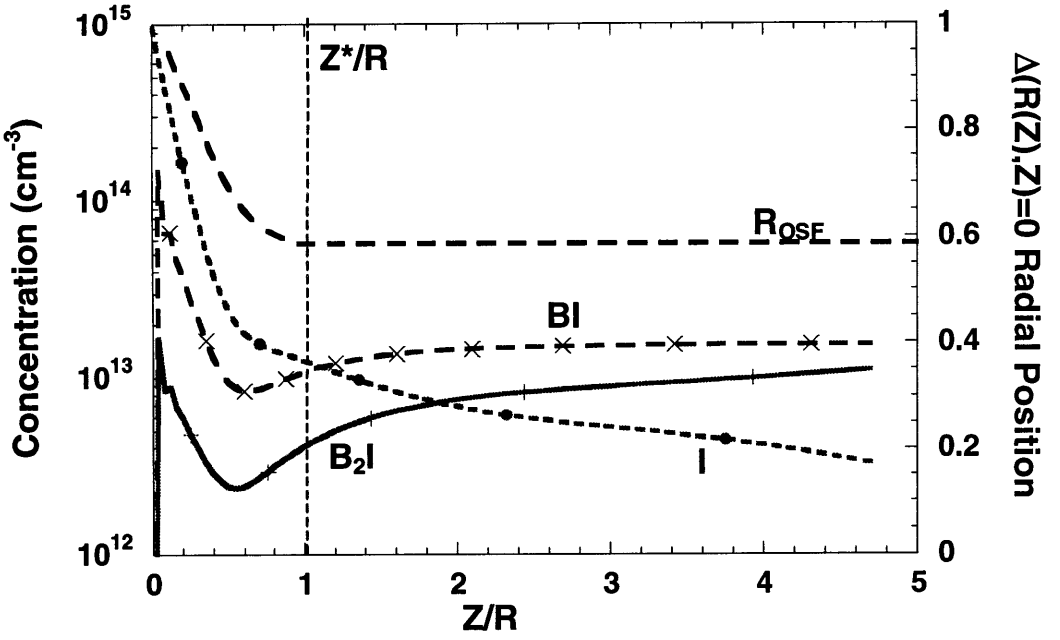

Figure 3-10

Concentration profiles of BI and I at R=0.8 and evolution of the OSF-Ring.

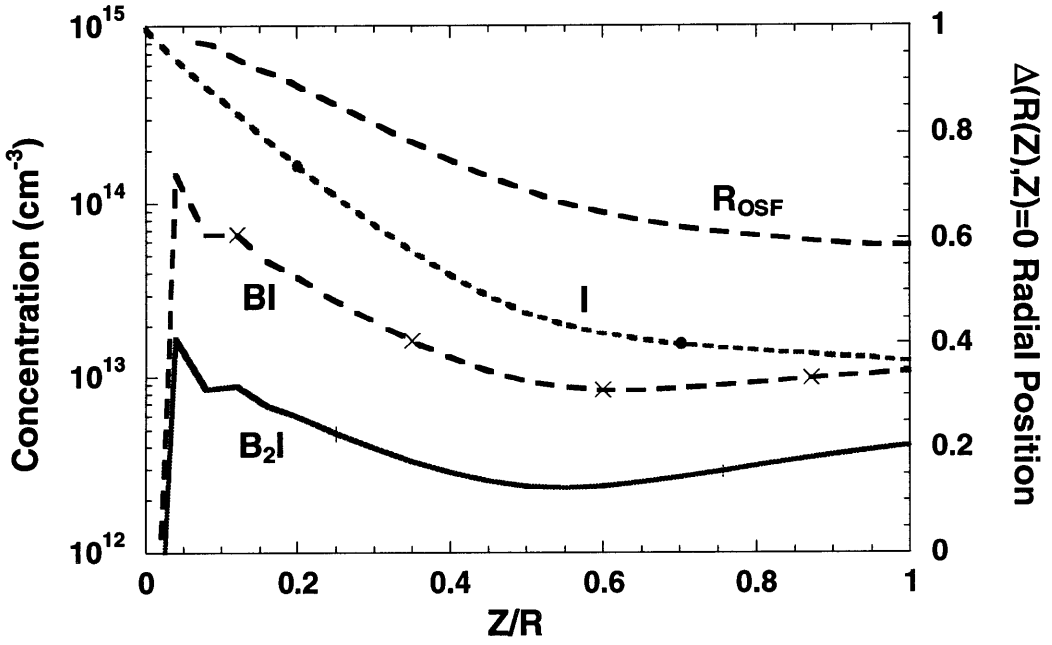

Figure 3-11

Concentration profiles of BI and I at R=0.8 and evolution of the OSF-Ring near melt-crystal interface.

3.2.2 BV

The BV concentration follows similar mechanism with BI by acting as a temporary vacancy storage, i.e. as internal source of vacancies. The vacancy release mechanism is illustrated in Figure 3-12. The peak of the BV concentration profile is on the order of $1x10^{13}$ cm^{-3}, and the same as with B_2I, while BI is on the order of 10^{14} cm^{-3}. A comparison of the order-of-magnitudes of the concentrations shows that the BI interstitial release mechanism is the dominant one and is the main reason for the shift in OSF-Ring position.

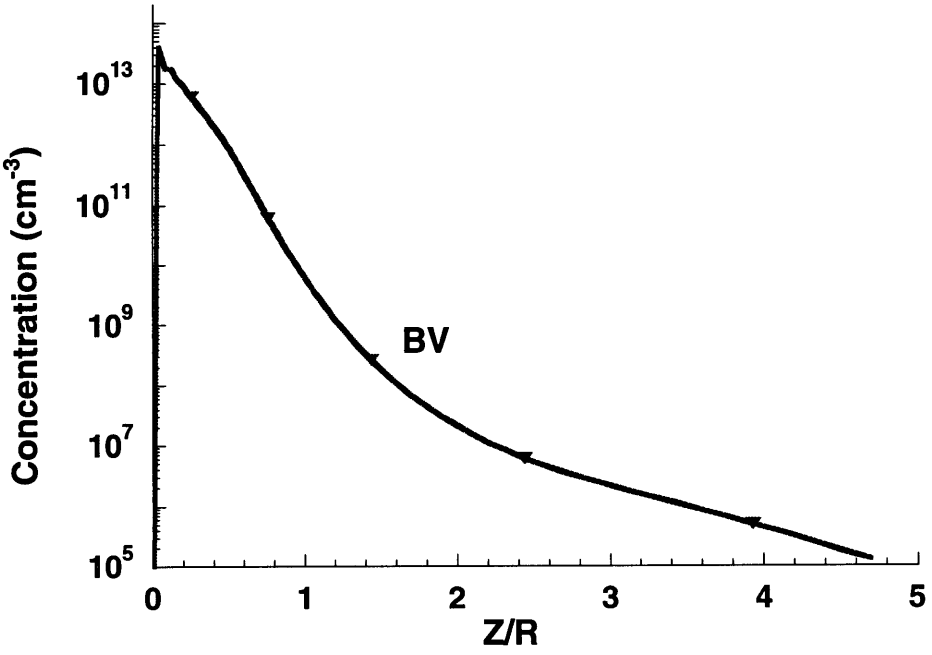

Figure 3-12

Axial concentration profile of BV at R=0.8.

3.2.3 Frank Turnbull Reaction

The Frank Turnbull reaction (Equation 2.7) depletes boron-interstitials and vacancies and, therefore, counters the vacancy release mechanism of BV. At the same time it reduces the effect of

BV formation and the release of interstitials by break up of BI. The Frank Turnbull reaction also depends on the availability of BI and V.

3.4 Parameter Sensitivity

Parameter sensitivity was used to analyze the binding enthalpies of BI and B_2I separately. A 15% increase of binding enthalpy was introduced in the best case described previously. By adjusting the binding entropy, the objective function was again minimized by adjusting the entropy to fit the experimental data. Fitting the results to the experimental data set using the microdefect model produce the following values shown in Table 3-2, with the binding energy values given at the melting temperature. With a 15% increase in H^b_{B2I}, χ was lowered from $4.76x10^{-3}$ to $3.70x10^{-3}$. For a 15% increase in H^b_{BI}, a higher value of χ was computed. The OSF-Ring positions as a function of boron concentration are shown in Figure 3-13 and 3-14. A change in binding enthalpy amplifies the change in binding entropy because the binding enthalpy is a more sensitive parameter. In conclusion, the sensitivity of binding enthalpy shows that an increase in binding enthalpy is compensated by reducing binding entropy to maintain the quality of the agreement between experiment and calculation.

Table 3-2

Analysis of binding enthalpy sensitivity of BI and B_2I.

Model Description	H^b_{BI} (eV)	S^b_{BI} (k_B)	H^b_{B2I} (eV)	S^b_{B2I} (k_B)	χ
Original Parameters	0.88	-5.98	1.18	-6.33	
Best Case	0.88	-0.44	1.18	-3.00	$4.76x10^{-3}$
15 % increase in H^b_{BI}	**1.01**	**-0.72**	1.18	-2.00	$5.92x10^{-3}$
15 % increase in H^b_{B2I}	0.88	-0.44	**1.35**	**-4.15**	$3.70x10^{-3}$

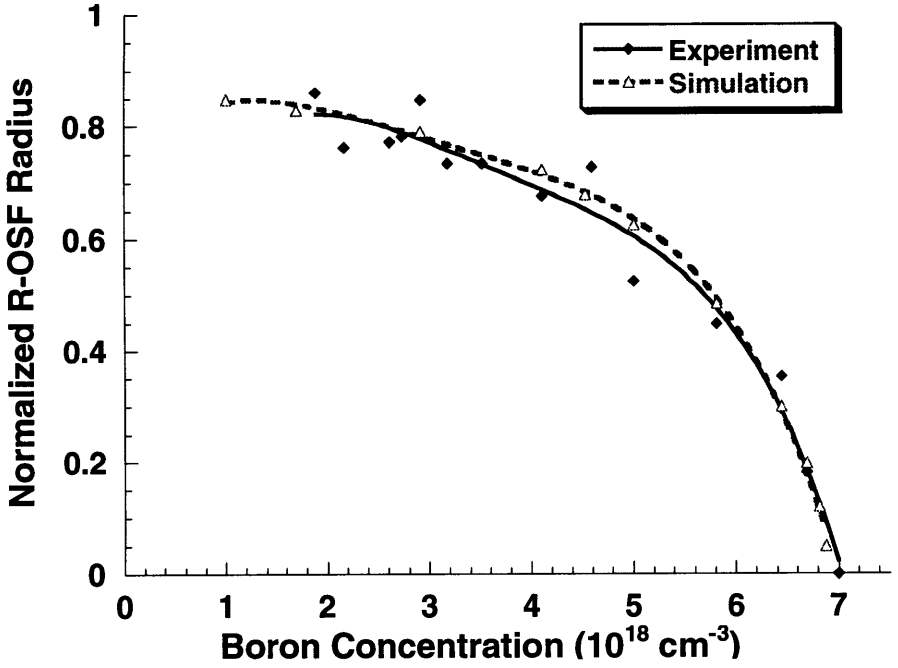

Figure 3-13

OSF-Ring position as a function of boron concentration with a 15% increase in the binding enthalpy of BI.

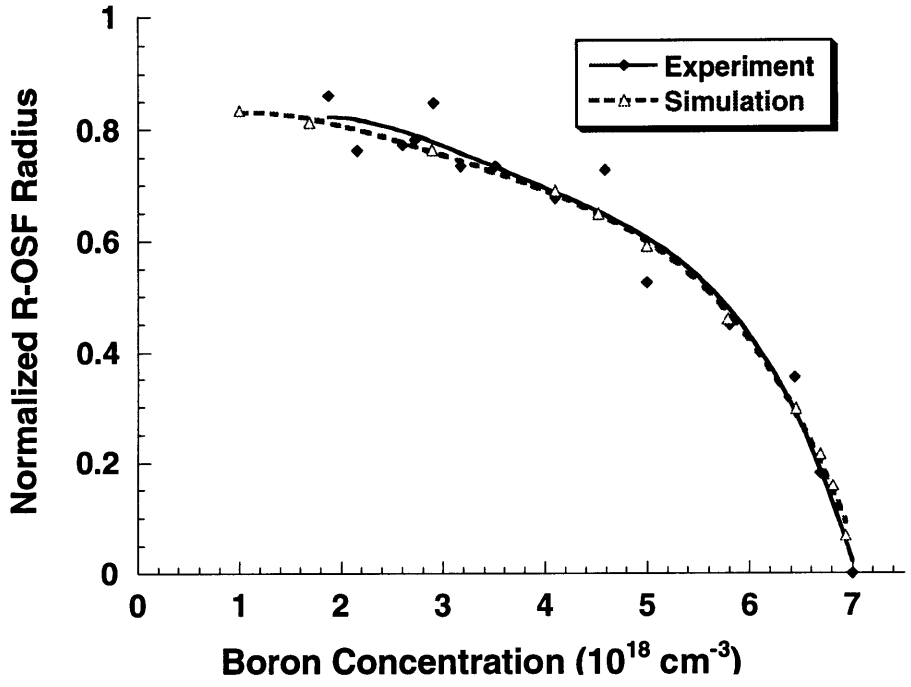

Figure 3-14

OSF-Ring position as a function of boron concentration with a 15% increase in the binding enthalpy of B_2I.

4. Conclusions

The formation of microdefects in silicon crystal appears to be controlled by the formation and dynamics of native point defects, namely self-interstitials and vacancies, which, it allowed to appear in excess, cluster to form either microvoids (vacancies) or stacking faults (interstitials). The point defect model of Sinno (1998) captures this dynamics and predicts the location of the OSF-Ring as the neutral region formed in a Czochralski crystal at the radial transition for a vacancy rich inner core to an interstitial dominated outer ring. In this thesis, the model of point defect dynamics has been extended to include the interactions of boron with point defects in order to predict the variation of the OSF-Ring diameter with boron concentration. The modeling is motivated by experimental results of Dornberger et al. (1997) that show a decrease in OSF-Ring radius with increasing boron concentration.

Our model for boron-point defect dynamics is based on Empirical Tight Binding analysis of the most stable boron/point defect complexes and diffusion limited reaction theory. The model quantitatively predicts the observed decrease in the OSF-Ring radius with only a modest amount of parameter fitting. The reactions included in the model are:

$$I + V \leftrightarrow 0, \tag{4.1}$$

$$B + B \leftrightarrow B_2, \tag{4.2}$$

$$B + I \leftrightarrow BI, \tag{4.3}$$

$$B_2 + I \leftrightarrow B_2I, \tag{4.4}$$

$$B + V \leftrightarrow BV, \tag{4.5}$$

$$BI + V \leftrightarrow B. \tag{4.6}$$

The validity of the chemical pumping mechanism (Hu, S.M., 1994) is supported by the mechanisms of BI, BV and B_2I in this microdefect model. These boron complexes act as traps for a short amount of time which slow intrinsic point defect diffusion and recombination and then release the point defect back into crystal. At high temperature range near the melt-crystal interface, the OSF-Ring is still dynamically moving within a short axial distance. Furthermore, the model for boron diffusion is governed by the formation of boron complexes (BI, B2I and BV) and by the

Frank Turnbull reaction. This means that the kick-out mechanism, especially involving the BI, is dominant.

The fitting of the predictions to experimental data is only accomplished for single specific thermal field and crystal shape is simulated for fit to experimental data. Experimental data from the widest possible set of conditions should be used to test the microdefect model further and to obtain more accurate microdefect model. The fitting mainly distributes the release mechanism for interstitials between the BI and B_2I mechanisms. Despite the two different weights for the two reactions, the model predictions were reasonably well fit to experimental data. Sensitivity analysis of the binding entropies has shown that the stability of either BI or B_2I depends more strongly on the binding enthapies.

The mechanism of boron diffusion is not completely understood and other defect species may exist. Further study of the microscopic behavior of boron in silicon is still important to understand its role in microdefect formation during crystal growth.

Appendices

Appendix A

Derivation of Equilibrium Constant Expression in term of Binding Energy

The derivation presented here is the equilibrium concentration of BI. Other equilibrium concentrations (B_2, B_2I, and BV) are derived similarly.

Starting from the equilibrium concentration of boron-interstitial in term of formation energy

$$K_{BI}^{eq} = \theta_{BI} \exp\left\{\frac{S_{BI}^{f}}{k_B}\right\} \exp\left\{-\frac{H_{BI}^{f}}{k_B T}\right\},$$

$$C_{BI}^{eq} = \theta_{BI}\, C_{B}^{eq} \exp\left\{\frac{S_{BI}^{f}}{k_B}\right\} \exp\left\{\frac{H_{BI}^{f}}{k_B T}\right\}.$$

Utilizing the binding entropy and binding enthalpy definition,

$$E_{BI}^{b} = E_{B}^{f} + E_{I}^{f} - E_{BI}^{f},$$

$$S_{BI}^{b} = S_{BI}^{f} - S_{B}^{f} - S_{I}^{f},$$

with E^f_B and S^f_B zero (the reference state), and substituting those binding energies in the equilibrium concentration expression into the equilibrium concentration of the boron-interstitial:

$$C_{BI}^{eq} = \theta_{BI}\, C_{B}^{eq} \exp\left\{\frac{S_{BI}^{b}}{k_B}\right\} \exp\left\{\frac{S_{I}^{f}}{k_B}\right\} \exp\left\{\frac{E_{BI}^{b}}{k_B T}\right\} \exp\left\{-\frac{E_{I}^{f}}{k_B T}\right\}.$$

The equilibrium concentration of interstitial is defined as:

$$C_{I}^{eq} = C_{s} \exp\left\{\frac{S_{I}^{f}}{k_B}\right\} \exp\left\{-\frac{E_{I}^{f}}{k_B T}\right\}.$$

The final equilibrium expression can be expressed in term of binding enthalpy and binding entropy as follows:

$$C_{BI}^{eq} = \frac{C_B^{eq} C_I^{eq}}{C_s} \theta_{BI} \exp\left\{\frac{S_{BI}^b}{k_B}\right\} \exp\left\{\frac{E_{BI}^b}{k_B T}\right\},$$

$$K_{BI}^{eq} = \theta_{BI} \exp\left\{\frac{S_{BI}^b}{k_B}\right\} \exp\left\{\frac{E_{BI}^b}{k_B T}\right\}.$$

Appendix B

Energetic of Boron Complex Calculations

Binding energy calculations below were calculated at melting temperature.

$H^f_I(Tm)= 3.97$ eV $\quad\quad$ $S^f_I(Tm)= 7.88\ k_B$

$H^f_V(Tm)= 2.87$ eV $\quad\quad$ $S^f_V(Tm)= 2.24\ k_B$.

$E^b_{B_2} = 2\ E^f_B - E^f_{B_2} = 0 - (-0.8) = 0.8$ eV

$S^b_{B_2} = S^f_{B_2} - 2\ S^f_B = 2.75\ k_B - 0 = 2.75\ k_B$

$E^b_{BI} = E^f_B + E^f_I - E^f_{BI} = 0 + 3.97 - 3.1 = 0.87$ eV

$S^b_{BI} = S^f_{BI} - S^f_B - S^f_I = 1.9\ k_B - 0 - 7.88\ k_B = -5.98\ k_B$

$E^b_{B_2I} = E^f_{B_2} + E^f_I - E^f_{B_2I} = -0.8 + 3.97 - 2.0 = 1.17$ eV

$S^b_{B_2I} = S^f_{B_2I} - S^f_{B_2} - S^f_I = 4.3\ k_B - 2.75.\ k_B - 7.88\ k_B = -6.33\ k_B$

$E^b_{BV} = E^f_B + E^f_V - E^f_{BV} = 0 + 2.87 - 2.3 = 0.85$ eV

$S^b_{BV} = S^f_{BV} - S^f_B - S^f_V = 3.3\ k_B - 0 - 2.24\ k_B = 1.06\ k_B$

Note:

Formation enthalpies of boron complexes were computed based on Empirical Tight Binding calculations. The Stillinger Weber calculations have uncertainty in vibrational entropy values.

Bibliography

Armigliato, A., Nobili, D., Ostoja, P., Servidori, M., and Solmi, S., in *Semiconductor Silicon*, (1977), 638.

Baccus, B., Vandenbossche, E., and Lannoo, M., *J. Appl. Phys.*, **77** (1995), 5630.

Chao, H.S. et al., J. Appl. Phys., **79** (1996), 2352.

Dornberger E., Personal Communication, June 1998.

Dornberger E., Graf D., Suhren M., et al., *J. Cryst. Growth.,* **180** (1997), 343.

Dornberger et al., *J. Cryst Growth.*, **180** (1997b), 461.

Dornberger, E. and von Ammon, W., *J. Electrochem. Soc.*, **143** (1996), 1648.

Fair, R. B., *J. Electrochem. Soc.*, **122** (1975), 80.

Fahey, P.M., Griffin, P. B., and Plummer, J.D., *Rev. Mod. Phys.*, **61** (1989), 289.

Frank, F. C. and Turnbull, D., *Phys. Rev.*, **8** (1975), 319.

Gossmann, H. J. et al., *Appl. Phys. Lett.*, **71** (1997), 3862.

Hu, S. M., *Mat. Sci. and Eng.*, **13** (1994), 105.

Inada, T., Kuranouchi, A., Hirano H., Nakamura, T., Kiyota, Y, and Onai, T., *Appl. Phys. Lett.,* **58** (1991), 1748.

Kingery, W. D., Bowen, H. K., and Uhlmann, D. R., *Introduction to Ceramics*, John Wiley & Sons, New York, 1976.

Luo, W. W., Rasband, P.B., and Clancy P., *J. Appl. Phys.*, **84**, 1998.

Mathiot, D., and Pfister, J. C., *J. Appl. Phys.*, **55** (1984), 3524.

Nichols, C.S., Van de Walle, C. G., and Pantelides S. T., *Phys. Rev. B*, **40** (1989), 6085.

Orr Arienzo et al., *J. Appl. Phys.*, **63** (1998), 116.

Rasband, P.B., Clancy, P., and Thompson, M. O., *J. Appl. Phys.*, **79** (1996), 95.

Rasband, P. B., Horsfield, A. P., and Clancy, P., *Philos. Mag. B*, **73**, (1996b), 71.

Sinno, T. R., (1998). *Defects in Crystalline Silicon: Integrated Atomistic and Continuum Modeling* Ph.D thesis, Massachusetts Institute of Technology.

Tan, T. Y., and Gosele, U., *J. Appl. Phys. A*, **37** (1985), 1.

Tang, M., Colombo, L., Zhu, J., and de la Rubia, T.D., *Phys. Rev. B*, **55** (1997), 14279.

Uematsu, M., *Jpn. J. Appl. Phys.*, **36** (1997), 7100.

Vandenbossche, E., and Baccus, b., *J. Appl. Phys.*, **73** (1993), 7322.

von Amon, W., Dornberger E., Oelkrug, H., and Weidner, H., *J. Crystal Growth*, **151** (1995), 273.

Voronkov, V. V., *J. Crystal Growth*, **59** (1982), 625.

Wolf, S. and Tauber, R. N., *Silicon Processing for the VLSI Era, Volume 1-Process Technology*, Lattice Press, California, 1986

Yamagishi, H., Fusegawa, I., Fujimaki, N., and Katayama, M., *Semicond. Sci. Technol.*, **7** (1992), A135.

Zhu, J. Diaz de la Rubia, T., Yang, L. H., Mailiot, C., and Gilmer, G. H., *Phys. Rev. B.*, **54** (1996), 4741.